https://doi.org/10.5194/esd-2020-63
Preprint. Discussion started: 19 August 2020

Earth System Dynamics Discussions

The sensitivity of the ENSO to volcanic aerosol spatial distribution in the MPI large ensemble

Benjamin Ward[1], Francesco S.R. Pausata[1], Nicola Maher[2]

[1] Département des sciences de la Terre et de l'atmosphère, Université du Québec à Montréal, Montréal, Canada
[2] Max-Planck-Institute for Meteorology, Hamburg, Germany

Correspondence to: Benjamin Ward (ward_soucy.benjamin@courrier.uqam.ca)

Abstract. Using the Max Planck Institute Grand Ensemble (MPI-GE) with 200 members for the historical simulation (1850-2005), we investigate the impact of the spatial distribution of volcanic aerosols on the ENSO response. In particular, we select 3 eruptions (El Chichón, Agung and Pinatubo) in which the aerosol is respectively confined to the Northern Hemisphere, the Southern Hemisphere or equally distributed across the equator. Our results show that the ENSO anomalies start at the end of the year of the eruption and peak the following one. Especially, we found that when the aerosol is located in the Northern Hemisphere or is symmetrically distributed, El Niño-like anomalies develop while aerosol distribution confined to the Southern Hemisphere leads to a La Niña-like anomaly. Our results strongly point to thevolcanically induced displacement of the ITCZ as the main mechanism that drives the ENSO response, while suggesting that the other mechanisms (the ocean dynamical thermostat, the cooling of tropical northern Africa or of the Maritime continent) commonly invoked to explain the post-eruption ENSO response appear not to be at play in our model.

1 Introduction

Aerosol particles from volcanic eruptions are the largest non-anthropogenic radiative forcing that have influenced the climate system in the past centuries (Robock, 2000). Oxidised, sulfur gases (mainly in form of SO_2) injected into the stratosphere by large Plinian eruptions form sulfate aerosols (H_2SO_4) (Pinto et al. , 1989; Pollack et al., 1976) that have a time residence of 1-3 years (Barnes & Hofmann, 1997; Robock & Yuhe Liu, 1994). These particles both scatter and absorb incoming solar radiation as well as part of the outgoing longwave radiation (Stenchikov et al., 1998; Timmreck, 2012). For intense and sulfur-rich volcanic eruptions, the net effect is a general cooling of the surface and a warming in the stratosphere where the aerosols tend to reside longer (Harshvardhan, 1979; Rampino & Self, 1984). The maximum global cooling is in general reached within 6-8 months following the eruption peak in optical depth before returning to normal values after about 3 to 4 years (Thompson et al., 2009). These rapid modifications in temperature can induce dynamic changes in the atmosphere and in the ocean including a strengthening of the polar vortex (e.g., Christiansen, 2008; Driscoll et al. , 2012; Kodera, 1994; Stenchikov et al., 2006), a weakening in the African and Indian Monsoon (e.g., Iles et al., 2013; Man et al., 2014 ; Trenberth & Dai, 2007;

https://doi.org/10.5194/esd-2020-63
Preprint. Discussion started: 19 August 2020


Earth System Dynamics Discussions

Zambri & Robock, 2016) as well as forced changes on the El Niño-Southern Oscillation (ENSO) (e.g., Emile-Geay et al., 2008; McGregor & Timmermann, 2011; Pausata et al., 2015; Wang et al., 2018).

Paleoclimate archives and observations from the past centuries suggested that large tropical eruptions are usually followed by a warm sea-surface temperature (SST) anomaly in the Pacific (El Niño events ; e.g., Adams et al. , 2003; D'Arrigo et al. , 2005; Li et al., 2013; S. McGregor et al. , 2010; Wilson et al., 2010). In particular, El Niño events followed in the first or the second winter after the five largest eruptions of the last 150 years (Krakatoa in August 1883, Santa Maria in October 1902, Agung in March 1963, El Chichón in April 1982 and Pinatubo in June 1991). However, the Santa Maria, El Chichón and Pinatubo eruptions occurred after an El Niño event was already developing making it difficult to determine a causal link between ENSO and these eruptions (e.g., Self et al., 1997; Nicholls, 1988).

Moreover, modelling studies initially found divergent responses for the ENSO changes after large tropical eruptions (Ding et al., 2014; McGregor & Timmermann, 2011; Stenchikov et al., 2006; Zanchettin et al., 2012). However, the most recent studies have pointed to an El Niño-like response following volcanic eruption (McGregor et al, in press). In particular, the use of relative sea surface temperature (RSST) or sea surface height (SSH) instead of SST have helped to disentangle the ENSO response from volcanically induced cooling in the Pacific and to highlight the dynamical ENSO response (Khodri et al., 2017; Maher et al., 2015).

Although a consensus is emerging, different aerosol spatial distributions may give rise to different ENSO responses. Stevenson et al., (2016) investigated the impact of NH, SH and tropical volcanic eruptions using the Community Earth System Model (CESM 1.1) Last Millennium Ensemble. They concluded that while NH and tropical eruptions tend to favour El Niño-like conditions, SH eruptions enhance the probability of La Niña events within one year following the eruptions. Conversely, Liu, Li, et al., (2018) through a millennium simulation performed with CESM 1.0 and Zuo et al., (2018) using the Community Earth System Model Last Millennium Ensemble (CESM-LME) concluded that SH, NH and tropical eruptions all resulted in El Niño-like conditions in the second year after the eruption.

The mechanisms that trigger a change in the ENSO state following volcanic eruptions is still debated. One of the most frequently used hypotheses is the "ocean dynamical thermostat" mechanism (ODT) (Clement et al., 1996), where a preferential cooling in the western Pacific relative to the eastern Pacific takes place due to the underlying dynamics of the Pacific Ocean. Such a differential cooling weakens the zonal SST gradient along the equatorial Pacific which causes a relaxation of the trade winds, leading to a temporary weakening of the ocean upwelling in the eastern Pacific. This process is then amplified by the Bjerknes feedback, yielding an El Niño (Bjerknes, 1969). A related mechanism for the preferential El Niño anomalies following volcanic eruptions is based on the recharge-discharge theory of ENSO, including changes I n the wind stress curl during the eruption year as one of the triggering factors (McGregor & Timmermann, 2011; Stevenson et al. 2017). However, through a set of sensitivity experiments, Pausata et al., (2020) have questioned the existence of the ODT mechanism in coupled

https://doi.org/10.5194/esd-2020-63
Preprint. Discussion started: 19 August 2020


Earth System Dynamics Discussions

climate models following volcanic eruptions, pointing to the Intertropical convergence zone (ITCZ) displacement and extratropic-to-tropic teleconnections as key mechanisms in affecting post-eruption ENSO. The ITCZ-shift mechanism was originally proposed for the ENSO response to high-latitude eruptions (Pausata et al., 2015; 2016) and then suggested to also be at work for tropical asymmetric eruptions (Colose et al., 2016; Stevenson et al., 2016). In general, the ITCZ shift away from the hemisphere that is cooled (Kang et al., 2008; Schneider et al., 2014). Consequently, for an eruption with aerosol concentrated in the NH, the ITCZ location moves equatorward, weakening the trade winds and leading to an El Niño-like anomaly via the Bjerknes feedback (Bjerknes, 1969). In contrast, the ITCZ moves northward following a larger SH cooling, strengthening the trade winds and triggering La Niña-like anomalies as seen in Colose et al. (2016) and Stevenson et al. (2016). Khodry et al. (2017) have invoked atmospheric teleconnections associated with the volcanically induced cooling of tropical Africa and weakening of the West African monsoon, which alter the Walker circulation, as the primary cause of the post-eruption El Niño-like anomalies. A similar mechanism has been suggested based on the cooling of the Maritime continent or south-eastern Asia instead of tropical Africa (Eddebbar et al., 2019; Ohba et al., 2013; Predybaylo et al.,2017). However, there is yet no consensus as to which of these proposed mechanisms is the main driver of the ENSO response after large volcanic eruptions.

Modeling studies have investigated the impact of volcanic eruptions on ENSO using different approaches. Many studies have used a superposed epoch (SEA) or composite analysis, in which they used a window of a few years before the eruption to create a reference to compare with the post-eruption period (e.g. Liu, Li, et al., 2018; Zuo et al., 2018). The significance of the response to volcanic eruptions is then assessed using a Monte Carlo method. However, this statistical methodology has some shortcomings as it is not able to fully remove the signal of internal variability: ENSO anomalies can still be seen in the reference period (see for example figure 4 in Liu, Li, et al., (2018)). Other studies use a limited number of ensemble members with the volcano and no-volcano members starting from different initial conditions (e.g. McGregor & Timmermann, 2011; Predybaylo et al., 2017; Sun et al., 2019). However, when starting the two ensemble sets from different initial conditions, a large number of ensemble members (equivalent to at least 150 years reference period/climatology) is needed to isolate the internal variability of ENSO (Milinski et al., 2019; Wittenberg, 2009). Here, for the first time, we use a 200-member ensemble taken from the Max Planck Institute Grand Ensemble (MPI-GE) for the historical simulations (1850-2005) (Maher et al., 2019) to investigate the ENSO response to hemispherically symmetric and asymmetric volcanic eruptions. The large ensemble and the different aerosol distributions allow us to shed light on the mechanisms at play in altering the ENSO state after volcanic eruptions.

2 Methodology and Experimental Design

In this study we consider the three largest eruptions of the last 100 years; the Agung in Indonesia (8 °S 115 °E) in February 1963; El Chichón in Mexico (17 °N 93 °W) in March 1982; and the Pinatubo in the Philippines (15 °N 120 °E) in June 1991. Two eruptions have an asymmetrical aerosol distribution, so either the aerosols are confined to the NH (El Chichón) or to the SH (Agung). The Pinatubo eruption has a symmetrical distribution with the sulfate aerosols spread across both hemispheres.

https://doi.org/10.5194/esd-2020-63
Preprint. Discussion started: 19 August 2020


Earth System Dynamics Discussions

We also considered the eruption of the Krakatoa in Indonesia (6 °S 105 °E) in 1883 which also produced a symmetrical aerosol plume to further corroborate our results. For clarity, we only show the results for Pinatubo, which are qualitatively similar to Krakatoa. The results of Krakatoa are displayed in the supplementary material (Figs. A7, A8 and A9).

We use 200 ensemble members of the historical simulations (1850-2005) performed using the Max Plank Institute for Meteorology Earth System Model 1.1 (MPI-ESM 1.1) (Giorgetta et al., 2013) as part of the Max Planck Institute Grand Ensemble (Maher et al., 2019). Such a large ensemble also allows us to analyse the ENSO response of individual eruptions instead of a composite of multiple eruptions as done in previous studies that used a limited number of ensembles (e.g. Maher et al., 2015; Stevenson et al., 2016; Zuo et al., 2018). All the ensemble members are initialized from different years of a long preindustrial control run (2000 years) after it has reached a quasi-stationarity state. The model horizontal resolution is roughly 1.8° for the atmosphere and 1.5° for the ocean with 16 vertical levels for both the atmosphere and the ocean.

The anomalies calculated are the difference between the reference (3 years before the eruption, which represents a total of 600 years climatology) and periods after the eruption. A Student t-test is used to estimate the significance of the mean changes before and after the eruptions at the 95% confidence level.

Large tropical eruptions induce a global cooling so that El-Niño response may be partly masked, and the La-Niña response amplified (Maher et al., 2015). Furthermore, some climate models amplify the volcanically induced cooling (e.g. Anchukaitis et al., 2012; Stoffel et al., 2015). To better highlight the dynamical changes, we remove the tropical SST mean from the original SST, this is known as the relative sea surface temperature (RSST) (Vecchi & Soden, 2007). In this study, we use the RSST to isolate the intrinsic ENSO signal (Khodri et al., 2017).

3 Results

3.1 ENSO response and its link to the ITZC-shift mechanism

The volcanic eruptions analyzed in the present study show three distinct aerosol plumes. While the aerosol distribution from the Pinatubo eruption is symmetrical around the equator, Agung and El Chichón eruptions both created to a large extent confined distribution in respectively the SH and the NH (Fig. 1). For the Pinatubo and El Chichón the aerosol optical depth peaks in the winter that follows the eruptions. For the Agung this maximum is reached in the winter of the second year after the eruption. These different distributions are due to the location of the volcanoes, the season and the strength of the eruption (Stoffel et al., 2015; Toohey et al., 2011).

Our simulations show an El Niño-like response to the El Chichón and Pinatubo eruptions and a La Niña-like response to the Agung eruption (Figs. 2 and 3). The ENSO anomalies develop at the beginning of the year after the eruption (Year 2) and then peak that boreal winter for El Chichón and Pinatubo or in the third boreal winter for Agung. The westerly anomalies in the trade winds are detected starting in the autumn of the eruption (Year 1). For all the eruptions, the relative Niño 3.4 index peaks

https://doi.org/10.5194/esd-2020-63
Preprint. Discussion started: 19 August 2020


Earth System Dynamics Discussions

in the winter of the year after the eruption reaching a maximum of approximately +0.3°C for El Chichón and the Pinatubo and a minimum of -0.2 °C for Agung (Fig. A3).

The asymmetric forcing caused by the three eruptions induces a different cooling of the surface temperature in the two hemispheres (Fig. 4). Although Pinatubo is the most intense eruption and has the largest global temperature decrease (Fig. A2), El Chichón shows the strongest hemispherical cooling (Fig. 4). The hemispherical cooling associated to Agung (SH) is in absolute values comparable to Pinatubo even if Agung's magnitude was twice as small (Bluth et al., 1992; Self & Rampino, 2012). Furthermore, while the aerosol distribution of the Pinatubo eruption is symmetric, the cooling is not and is concentrated in the NH, which is likely due to uneven distribution of landmass between hemispheres (i.e. reduced heat capacity in the NH). The maximum cooling for all three eruptions occurs at the beginning of year two and so does the temperature difference between the two hemispheres (Figs. 4 and A1).

Our results are consistent with the displacement of the Hadley cell associated with the differential cooling between the hemispheres, showing a northward shift of the ITCZ for the eruption of the Agung, and a southward shift for both El Chichón and the Pinatubo, for the three years following the eruption (Figs. 5 and 6). Additionally, the Pinatubo's rainfall anomaly is the largest even though the difference in the cooling of each hemisphere is stronger for El Chichón. This could indicate that the on-going global warming could amplify the rainfall anomaly following the volcanic eruptions through modulation in the ocean stratification and near-surface winds amplifying the response as suggested in a recent study (Fasullo et al., 2017) (Fig. A9). We find that the ITCZ displacement and associated rainfall anomalies peak the second year after the eruption, when the differential cooling of the hemisphere is larger (Figs. 4, 5 and 6). The ITCZ displacement is associated with a strengthening of the trade winds for the Agung eruption and a weakening for the El Chichón and Pinatubo eruptions as expected by the direction of the ITCZ movement in each case. These wind anomalies affect then the ENSO state: a change in the strength of the trade winds along the equatorial Pacific alters the ocean upwelling in the eastern side. This leads to a change in the east-west temperature contrast across the tropical Pacific, which is amplified by the Bjerknes feedback (Bjerknes, 1969) thus altering the ENSO state. All our results (the evolution of the Nino 3.4 index, the precipitation anomalies or the temperature anomalies) show an almost perfect symmetry between the tropical/NH distribution and the SH distribution (Figs. 2, 3, 4, 5, 6 and A2), which strongly suggests that the volcanically induced ITCZ displacement is the key mechanism to explain the ENSO response to the volcanic forcing in agreement with others studies (Colose et al., 2016; Pausata, et al., 2016; Stevenson et al., 2016; Pausata et al,. 2020).

3.2 ENSO response and its link to other mechanisms

The most commonly invoked mechanism that explains the ENSO response after large tropical volcanic eruptions is the ODT (Clement et al., 1996) and the preferential cooling of the warm pool relative to the eastern equatorial Pacific, leading to an El Niño-like response (e.g. Emile-Geay et al., 2008; Mann et al., 2005). However, in our simulations even if there is a volcanic aerosol over the equatorial Pacific and a surface cooling for all the eruptions (Figs. 1, A3, A4 and A5), we see a negative phase

https://doi.org/10.5194/esd-2020-63
Preprint. Discussion started: 19 August 2020


Earth System Dynamics Discussions

of ENSO and an anomalous easterly wind stress developing after the Agung eruption (Figs. 2 and 3). These results thus suggest that the ODT is not a dominant mechanism in our model.

Another mechanism often used to explain the post-eruption El Niño-like response is related to the cooling of the Maritime Continent first proposed by Ohba et al. (2013) and also suggested in recent studies (e.g.,Eddebbar et al., 2019) : the smaller heat capacity of the land in comparison to the ocean cause a stronger land cooling that reduces the temperature gradient between the Maritime Continent and the western Pacific Ocean. Such temperature changes lead to a weakening of the trade winds and an eastward shift of the rainfall (El Niño pattern). Our results show a cooling of the Maritime Continent and a reduction of the convective activity in the three eruptions (Figs. A3, A4 and A5). Nevertheless, our model simulates the development of a La Niña-like conditions after the eruption of the Agung (Figs. 1 and 2), which is at odds with the cooling of the Maritime Continent mechanism where El Niño-like conditions would be expected for all three eruptions.

Khodri et al., (2017) suggested that the cooling of tropical Africa, following volcanic eruptions, may increase the likelihood of an El Niño events through the weakening of the West African Monsoon and changes in the Walker circulation. More specifically, the reduction of the tropical precipitation favours atmospheric Rossby waves in the autumn season (SON) and a downwelling Kelvin wave that alters the Walker circulation and leads to El Niño-like conditions in the year after the eruption. Our results show a mixed response over Africa with Agung and Pinatubo both displaying a cooling (Figs. A3 and A5) but leading to different ENSO responses (Figs. 1 and 2). Moreover, after El Chichón eruption a warming of the tropical northern Africa takes place in the first year and an El Niño-like anomaly develops (Figs. 2, 3 and A4). Hence, in our model, the volcanically induced cooling of tropical Africa and the atmospheric perturbations associated with the suppression of the African monsoon seem not to play a critical role in altering the ENSO state following volcanic eruptions.

Recently, Pausata et al., (2020) proposed an additional mechanism related to the extratropical-to-tropical teleconnections that tends to favour an El Niño-like response for both NH and SH eruptions, hence playing in synergy (NH eruptions) or against (SH eruptions) the ITCZ-shift mechanism. However, our qualitative analysis of the sea level pressure (SLP) anomalies does not match the changes expected by this mechanism (cf. Fig. A10 to Fig. 4 (a-d) in Pausata et al., (2020)). In this recent study, the volcanic aerosol alters the meridional temperature gradient of the atmosphere that eventually causes a poleward shift of the Pacific jet stream and a strong cyclonic surface pressure anomaly over the midlatitude to subtropical Pacific basin in both NH and SH eruptions in the first summer following the eruptions. In our simulation, the response is opposite for the Agung and El Chichón or Pinatubo eruptions, suggesting more that the simulated extratropical anomalies are induced by the ENSO changes due to the eruption rather than affecting ENSO (Fig. A10). The reason of the disagreement could lie in the fact that the El Niño/La Niña-like response following the volcanic eruptions peak in the first winter in Pausata et al., (2020) modeling study, while in our model in the second winter (Figs. 2 and 3). The extratropical-to-tropical teleconnection could make the El Niño development following NH/symmetric eruptions occur faster than in our case where such a teleconnection appears not to be present. Ad hoc sensitivity experiments are necessary to rule out the above-mentioned mechanisms in our model.

https://doi.org/10.5194/esd-2020-63
Preprint. Discussion started: 19 August 2020


Earth System Dynamics Discussions

4 Discussion and conclusions

Our study used the largest ensemble simulation (200 ensembles) currently available of the historical period performed with the MPI-ESM model to better understand the impact of the volcanic eruptions on ENSO. Our results strongly point to the volcanically induced ITCZ displacement as the primary driver of the ENSO response following volcanic eruptions. In our simulations, the ENSO response after the eruptions critically depends on the distribution of the aerosol plume. When the volcanic aerosol distribution is confined to the NH or its distribution is symmetrical across the hemispheres the ENSO state tends towards a positive phase (El-Niño like conditions ; Fig. 2 (d-i)), while when the aerosols are confined to the SH the ENSO state is pushed towards a negative phase (La Niña-like conditions ; Figs. 2 (a-c)). The displacement of the ITCZ following the eruptions, caused by the asymmetric cooling of the hemisphere that pushes the ITCZ towards the hemisphere that is less cooled (Kang et al., 2008; Schneider et al., 2014). Both the eruptions with aerosol confined to the NH and symmetrically distributed across the hemispheres preferentially cool the NH, consequently shifting the ITCZ southwards, weakening the trade winds over the equatorial Pacific and triggering an El Niño like response through the Bjerknes feedback (Bjerknes, 1969). The eruption with the aerosol plume confined to the SH instead cools exclusively the SH, pushing the ITCZ northward and strengthening the trade winds, leading to a La Niña-like response.

The ITCZ mechanism we see at play in our model is supported by other recent studies performed with different climate models (Pausata,et al., 2015, 2020; Stevenson et al., 2016; Colose et al., 2016). Pausata et al. (2020) through a set of sensitivity experiments in which the volcanic aerosol forcing is confined to either the northern or the southern hemisphere show the key role of the ITCZ displacement in driving the ENSO response. They also highlighted the presence of another mechanism related to the extratropical-to-tropical teleconnections that no matter the type of eruption (NH or SH) tends to favour an El-Niño like response. Hence, it plays in synergy (NH eruptions) or against (SH eruptions) the ITCZ-shift mechanism. However, the simulated SLP changes in the extratropics in our model seem to be in response to the volcanically induced ENSO changes rather than affecting the ENSO response (cf. Fig. A10 to Fig. 4 (a-d) in Pausata et al., (2020)).

Our work also pointed out that the ODT (Clement et al., 1996), the cooling of the Maritime Continent (Ohba et al., 2013) and of the tropical Africa (Khodri et al., 2017) mechanisms are not at play. These previous studies that have suggested a different mechanism to explain the ENSO response to volcanic eruptions are based on a limited number of ensemble members (e.g. 5 members for 3 eruptions for the SH plume in Zuo et al. (2018)) or they heavily rely on statistical tools (e.g. SEA in Liu et al. (2018)). Consequently, those results may be biased by the use of a restrained number of ensemble members. Hence, our study points out the importance of a large number of ensemble members when investigating the ENSO response to volcanic eruptions. The absence of these mechanisms following volcanic eruptions is also in qualitative agreement with the modeling experiments in Pausata et al. (2020).

Finally, our results are consistent with the predominance of post-eruption El Niño events (Adams et al., 2003 McGregor et al, in press) and it can provide an explanation on why the majority of both observations and reconstructions are displaying El

https://doi.org/10.5194/esd-2020-63
Preprint. Discussion started: 19 August 2020

Niño events instead of La Niña events. However, the ENSO responses discussed in this study are only tendential (El Niño-like or La Niña-like response), i.e., intrinsic variability evolving toward a La Niña at the time of the eruption would not necessarily lead to a post-eruption El Niño event even for a NH or symmetrical eruption, but rather to a dampening of the ongoing La Niña. Furthermore, our model suggests the peak in ENSO anomalies to be on the second or third year after the eruption as in most modeling studies (Khodri et al., 2017; Lim et al., 2016; McGregor & Timmermann, 2011; Ohba et al., 2013; Stevenson et al., 2017), which is at odds with the reconstructions and observations that see a peak in ENSO anomalies in the winter following the eruption. The delayed ENSO response in our model simulations relative to reconstructions and observations may be related to the apparent lack of extratropical-to-tropical teleconnections (Pausata et al., 2020) that could favour El Niño-like response already on the first winter following the eruption.

In conclusions, our results provide further insights into the mechanism driving the ENSO response to volcanic eruptions, highlighting in particular the role of the ITCZ shift. However, further coordinated efforts with specific sensitivity studies are necessary to delve into the other proposed mechanisms and to unravel the difference between modeling studies and reconstructions with regards to the peak of the ENSO response. Given that ENSO is the major leading mode of tropical climate variability, which has worldwide impacts, these types of studies are also necessary to help improve seasonal forecasts following large volcanic eruptions.

https://doi.org/10.5194/esd-2020-63
Preprint. Discussion started: 19 August 2020

Earth System Dynamics Discussions
Open Access
EGU

Appendices

Appendix A

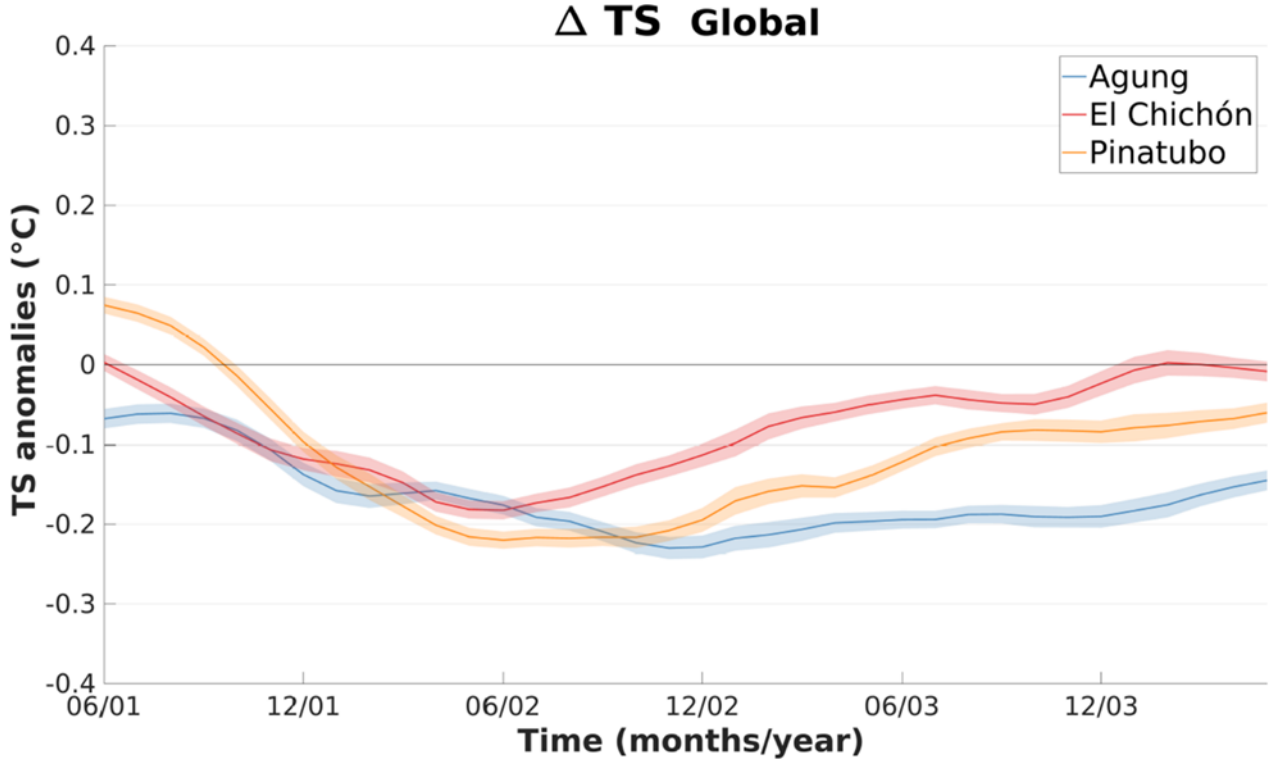

Figure A1: Evolution of the ensemble mean of the global the cooling in the three eruptions case for three years, starting at the first summer after the eruption. The 3-year climatology is subtracted to calculate the anomalies. Shading represents twice the standard error of the ensemble mean (i.e. ~95% confidence interval).

https://doi.org/10.5194/esd-2020-63
Preprint. Discussion started: 19 August 2020

Earth System Dynamics
Discussions
Open Access
EGU

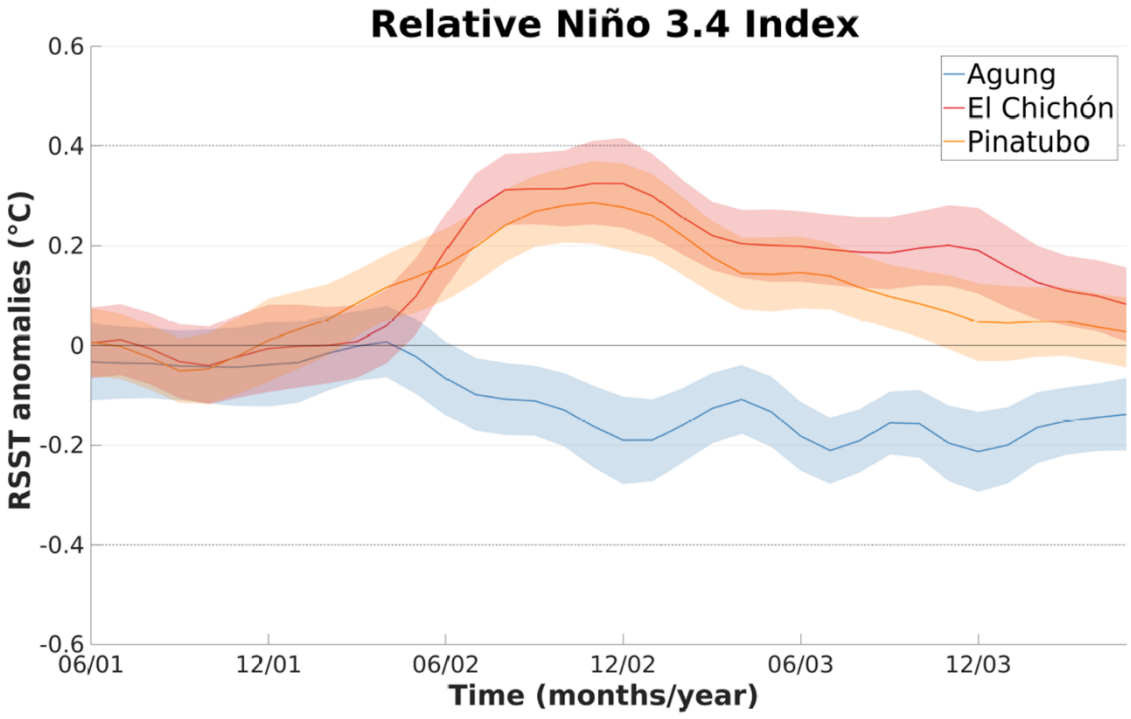

Figure A2: Ensemble mean changes in the relative Niño 3.4 index after each eruption. The 3-year climatology is subtracted to calculate the anomalies. Shading represent twice the standard error of the mean using an approximate 95% confidence interval.

https://doi.org/10.5194/esd-2020-63
Preprint. Discussion started: 19 August 2020

Earth System Dynamics
Discussions
Open Access
EGU

260

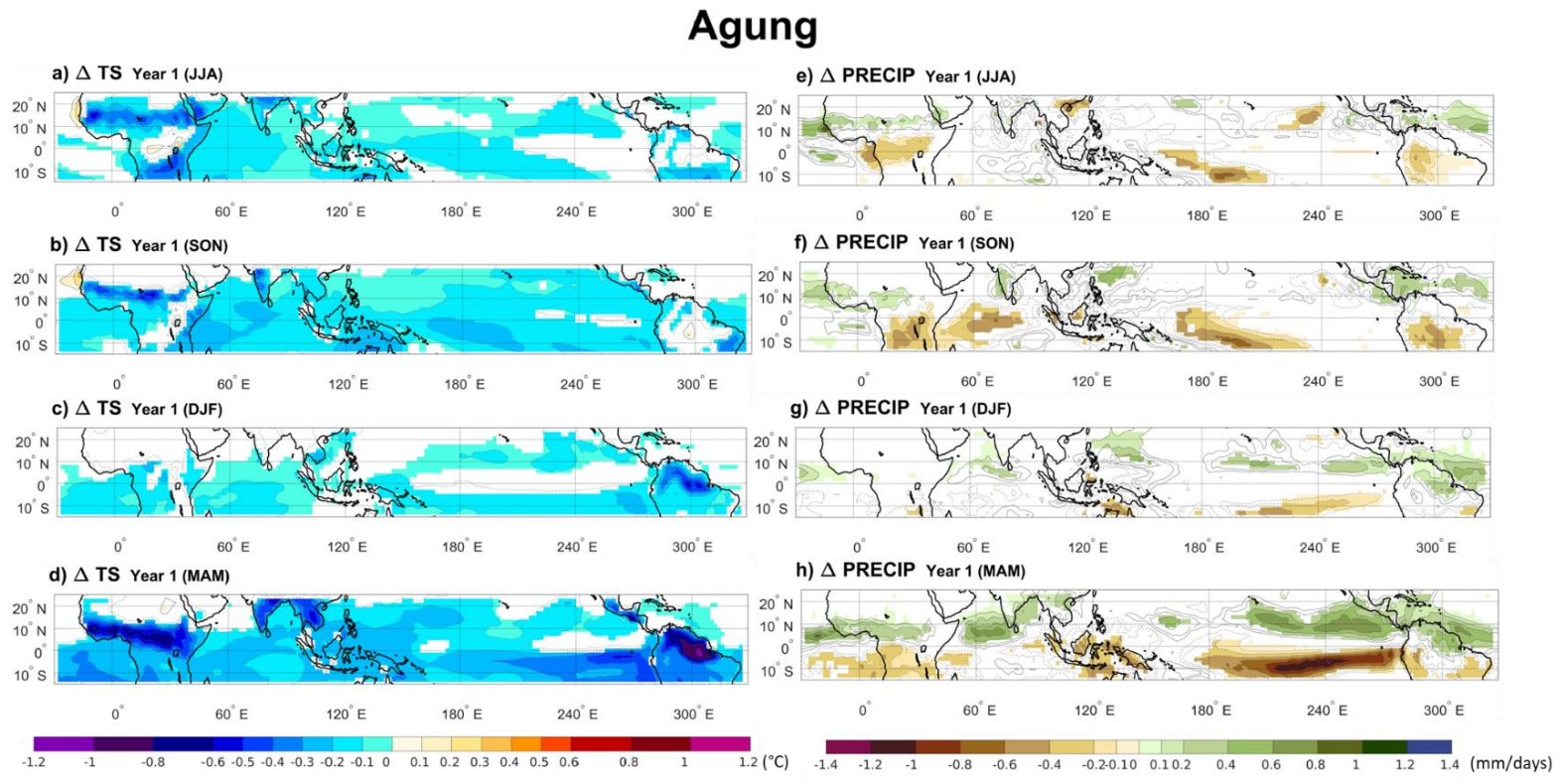

Figure A3: Ensemble mean of changes in surface temperature (a,b,c,d) and precipitation (e,f,g,h) between the climatology and the volcano case for each seasons of the year after Agung eruption. Only significant anomalies are showed with an approximate 95% confidence level using a Student *t*-test. Contour shows temperature and precipitations anomalies following the color bar scale (solid line for positive anomalies and dashed line for negative anomalies).

265

270

275

https://doi.org/10.5194/esd-2020-63
Preprint. Discussion started: 19 August 2020

Earth System Dynamics
Discussions
Open Access
EGU

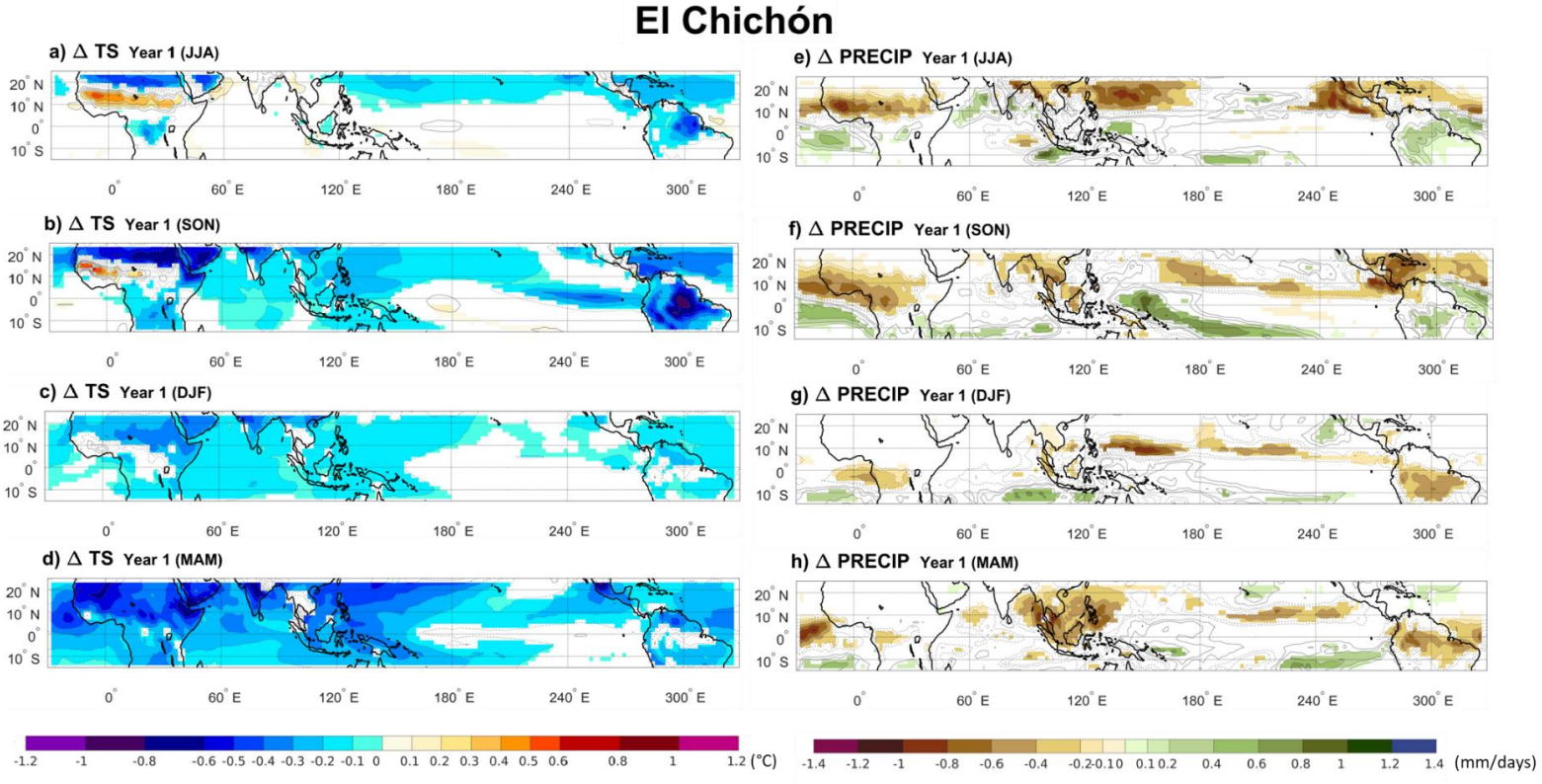

Figure A4: Ensemble mean of changes in surface temperature (a,b,c,d) and precipitation (e,f,g,h) between the climatology and the volcano case for each seasons of the year after El Chichón eruption. Only significant anomalies are showed with an approximate 95% confidence level using a Student *t*-test. Contour shows temperature and precipitations anomalies following the color bar scale (solid line for positive anomalies and dashed line for negative anomalies).

https://doi.org/10.5194/esd-2020-63
Preprint. Discussion started: 19 August 2020

Earth System Dynamics
Discussions
Open Access
EGU

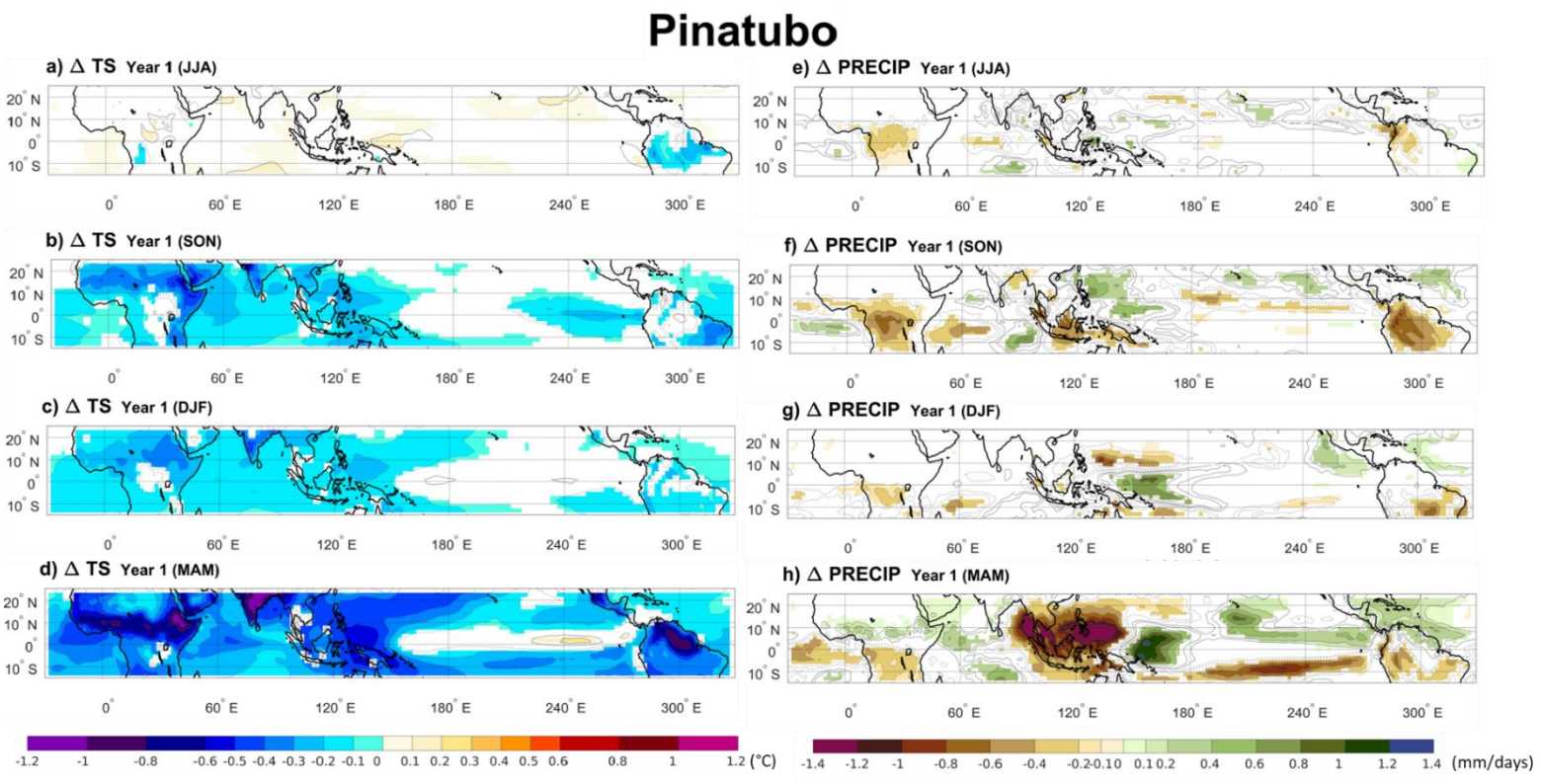

295

Figure A5: Ensemble meanof changes in surface temperature (a,b,c,d) and precipitation (e,f,g,h) between the climatology and the volcano case for each seasons of the year after Pinatubo eruption. Only significant anomalies are showed with an approximate 95% confidence level using a Student *t*-test. Contour shows temperature and precipitations anomalies following the color bar scale (solid line for positive anomalies and dashed line for negative anomalies).

300

305

310

https://doi.org/10.5194/esd-2020-63
Preprint. Discussion started: 19 August 2020

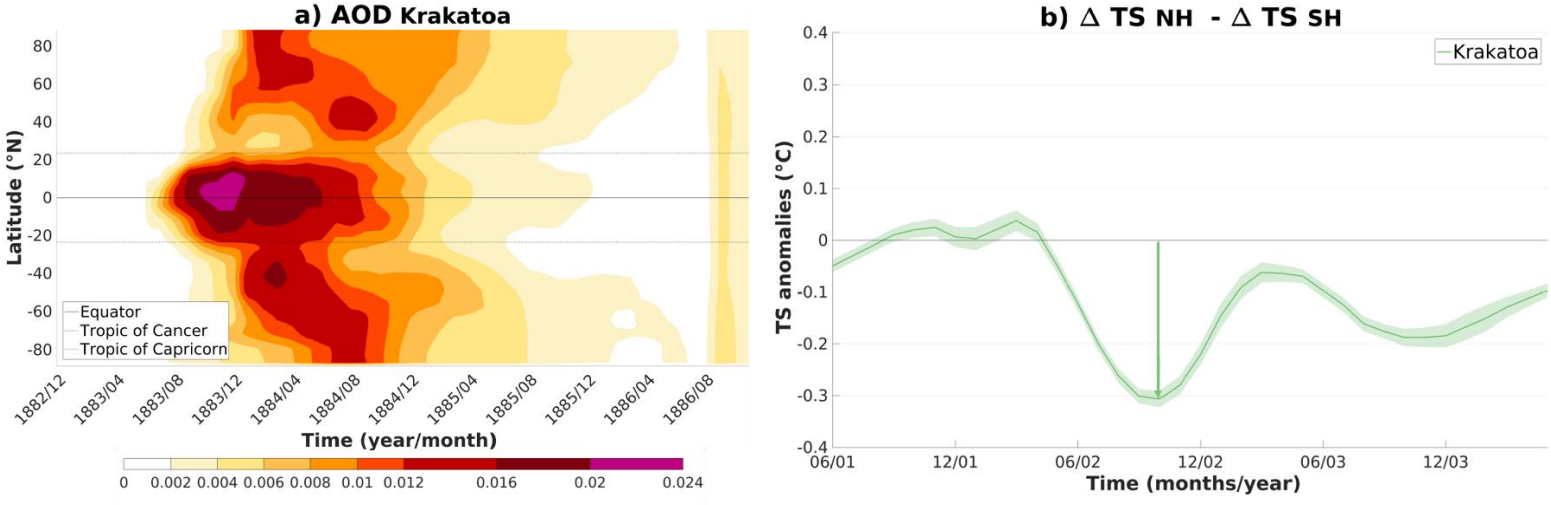

Figure A6: Evolution of the aerosol optical depth and ensemble average of the difference between the cooling of the SH (ΔT SH) and the NH (ΔT NH) for the Krakatoa eruption. (a) The band of wavelength used is between approximatively 555 nm and 675 nm. (b) 3-year climatology is subtrackedto calculate the anomalies. Shading represents twice the standard error of the ensemble mean (i.e. 95% confidence interval).

https://doi.org/10.5194/esd-2020-63
Preprint. Discussion started: 19 August 2020

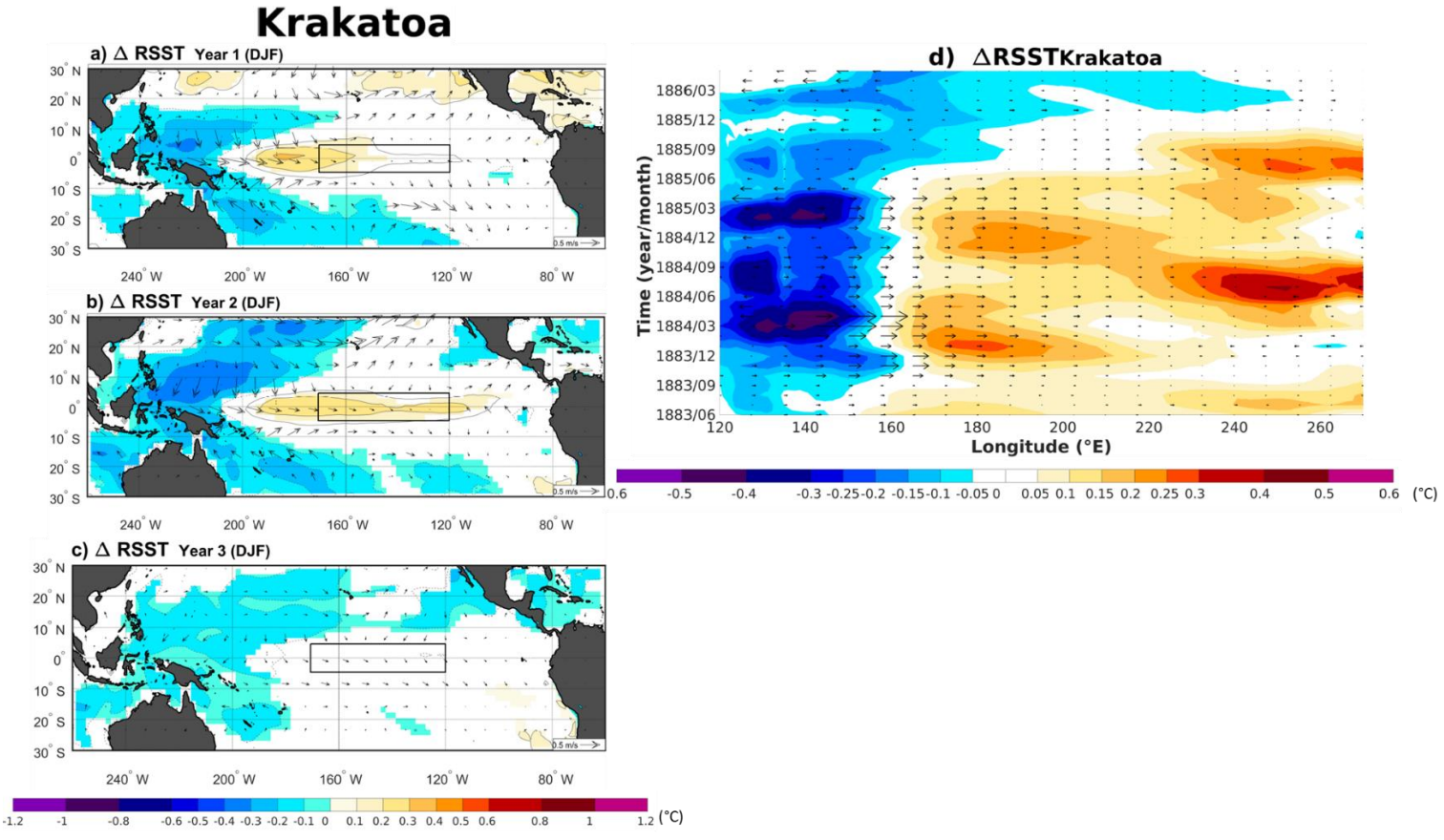

Figure A7: Ensemble mean of changes in relative sea surface temperature anomalies and 10m winds (arrows) between the climatology and the volcano case for the three-winter season (DJF) after the Krakatoa eruption. Only significant RSST changes are showed with an approximate 95 % confidence level using a Student *t*-test. Contours show the RSST anomalies following the color bar scale (solid lines for positive anomalies and dashed lines for negative anomalies). The boxes indicate the Niño 3.4 area.

https://doi.org/10.5194/esd-2020-63
Preprint. Discussion started: 19 August 2020

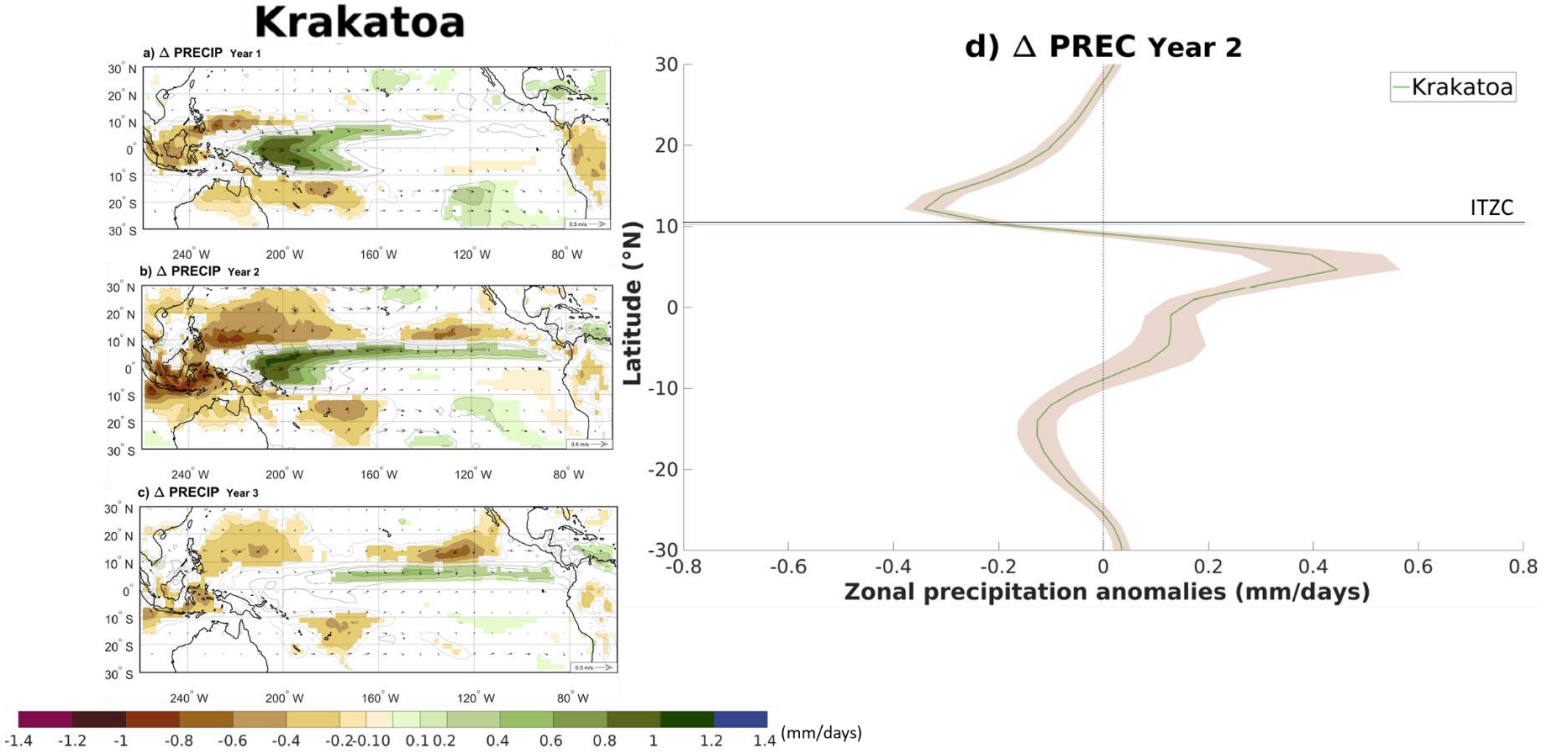

355 **Figure A8: (a), (b) ,(c) Ensemble mean of changes in precipitation and 10 m wind (arrows) between the 3-year climatology and the volcano case for the three summer to winter seasons (June to February) following the Krakatoa eruption. Only precipitation changes that are significant at the 95% confidence level using a Student *t*-test are shaded. Contours show the precipitation anomaly following the color bar scale (solid lines for positive anomalies and dashed lines for negative anomalies, the 0 line is omitted). (d) Ensemble average of the zonal precipitation anomaly over the Pacific Ocean (160 °E-100 °W) between the 3-year climatology and the summer**
360 **to winter season (June to February) of the second year after the Krakatoa eruption. Shading represents twice the standard error of the ensemble mean (i.e. ~95% confidence interval). The blue line highlights the ensemble-averaged 3-year climatology position of the ITCZ (defined as the location of the zonal-average precipitation maximum).**

365

370

https://doi.org/10.5194/esd-2020-63
Preprint. Discussion started: 19 August 2020

Earth System Dynamics
Discussions
Open Access
EGU

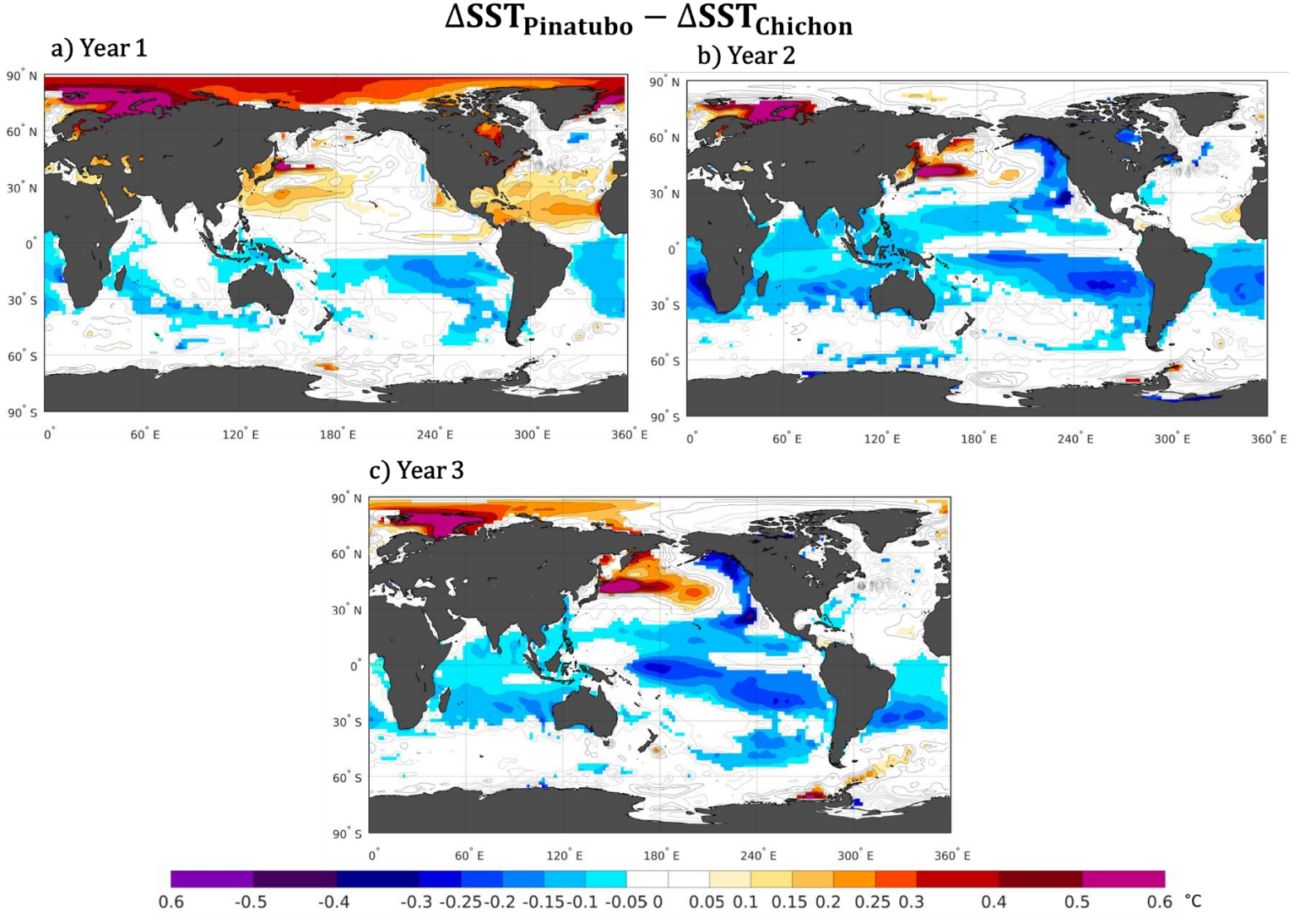

Figure A9: Difference in the ensemble mean sea surface temperature anomalies between the Pinatubo and El Chichón eruptions. ($\Delta TS_{Pinatubo}$- $\Delta TS_{Chichon}$). Only significant anomalies are showed with an approximate 95% confidence level using a Student *t*-test. Contour shows temperature anomalies following the color bar scale (solid line for positive anomalies and dashed line for negative anomalies).

https://doi.org/10.5194/esd-2020-63
Preprint. Discussion started: 19 August 2020

Earth System Dynamics
Discussions
Open Access
EGU

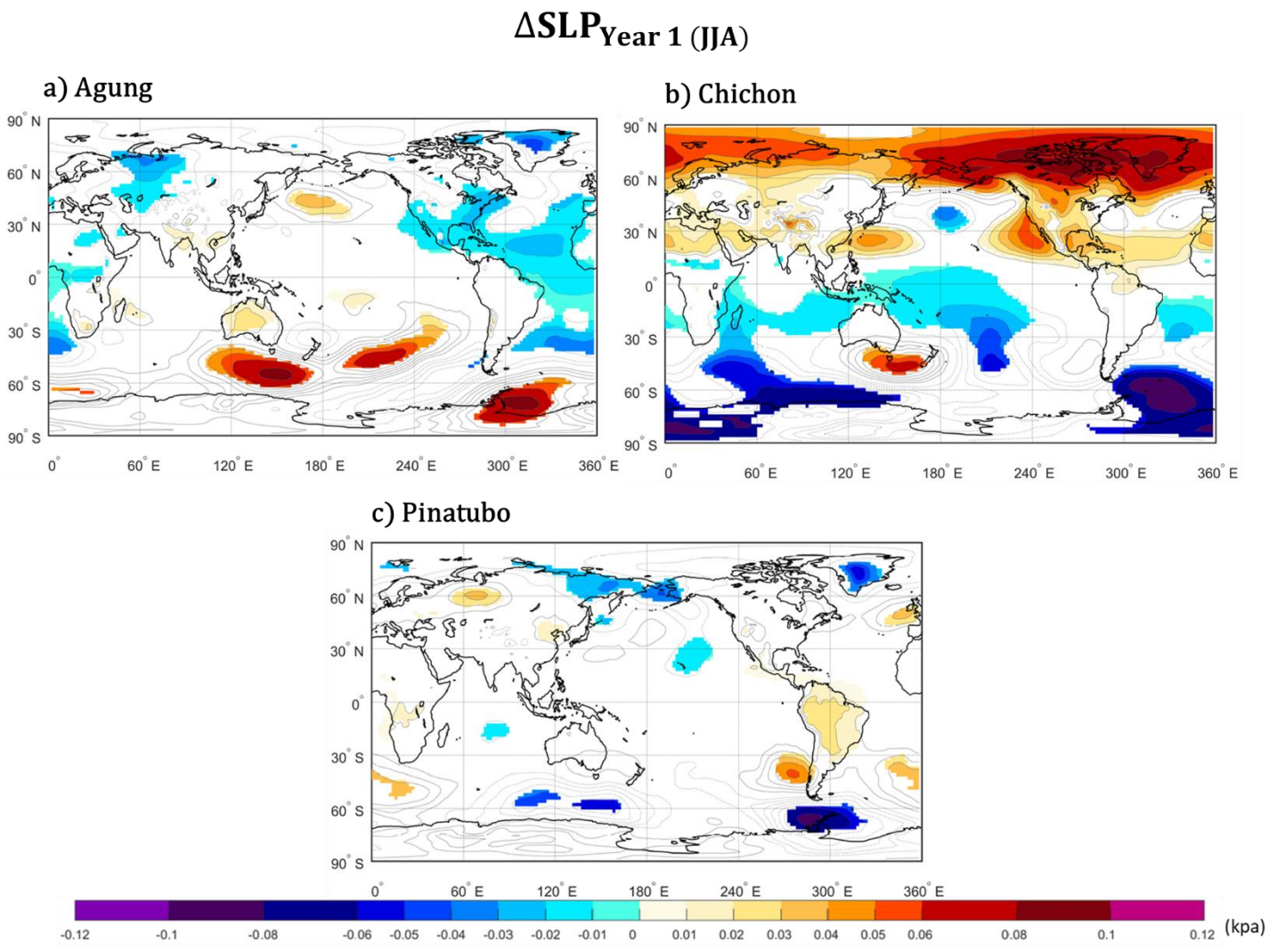

Figure A10: Ensemble average of change in the sea level pressure between the climatology and the volcano case for the first summer after Agung (a), El Chichón (b) and Pinatubo (c) eruptions. Only significant anomalies are showed with an approximate 95% confidence level using a Student *t*-test. Contour shows SLP anomalies following the color bar scale (solid line for positive anomalies and dashed line for negative anomalies).

https://doi.org/10.5194/esd-2020-63
Preprint. Discussion started: 19 August 2020

Author contribution

BW analysed the model output and wrote the manuscript with support of FSRP and NM. FSRP conceived of the presented ideas and supervised the findings of this work. NM provided the model output. All authors contributed to the interpretation of the results and the writing of the manuscript.

Competing interest

The authors declare that they have no conflict of interest.

Acknowledgements

We thank Mikhail Dobrynin and Johanna Baehr from the University of Hamburg for completing the second hundred MPI-GE ensemble simulations and providing the data from these simulations for use in this paper.
BW and FSRP acknowledge the financial support from the Natural Sciences and Engineering Research Council of Canada (grant RGPIN-2018-04981) and the Fonds de recherche du Québec–Nature et technologies (2020-NC-268559). NM was supported by the Max Planck Society for the Advancement of Science and the Alexander von Humboldt Foundation.

References

Adams, J. B., Mann, M. E. and Ammann, C. M.: Proxy evidence for an El Niño-like response to volcanic forcing, Nature, doi:10.1038/nature02101, 2003.

Anchukaitis, K. J., Breitenmoser, P., Briffa, K. R., Buchwal, A., Büntgen, U., Cook, E. R., D'Arrigo, R. D., Esper, J., Evans, M. N., Frank, D., Grudd, H., Gunnarson, B. E., Hughes, M. K., Kirdyanov, A. V., Körner, C., Krusic, P. J., Luckman, B., Melvin, T. M., Salzer, M. W., Shashkin, A. V., Timmreck, C., Vaganov, E. A. and Wilson, R. J. S.: Tree rings and volcanic cooling, Nat. Geosci., doi:10.1038/ngeo1645, 2012.

Barnes, J. E. and Hofmann, D. J.: Lidar measurements of stratospheric aerosol over Mauna Loa Observatory, Geophys. Res. Lett., doi:10.1029/97GL01943, 1997.

Bjerknes, J.: Monthly Weather Reyiew Atmospheric Teleconnections From the Equatorial Pacific, Mon. Weather Rev., 1969.

Bluth, G. J. S., Doiron, S. D., Schnetzler, C. C., Krueger, A. J. and Walter, L. S.: Global tracking of the SO2 clouds from the June, 1991 Mount Pinatubo eruptions, Geophys. Res. Lett., doi:10.1029/91GL02792, 1992.

Christiansen, B.: Volcanic eruptions, large-scale modes in the Northern Hemisphere, and the El Niño-Southern Oscillation, J. Clim., doi:10.1175/2007JCLI1657.1, 2008.

Clement, A. C., Seager, R., Cane, M. A. and Zebiak, S. E.: An ocean dynamical thermostat, J. Clim., doi:10.1175/1520-0442(1996)009<2190:AODT>2.0.CO;2, 1996.

Colose, C. M., LeGrande, A. N. and Vuille, M.: Hemispherically asymmetric volcanic forcing of tropical hydroclimate during the last millennium, Earth Syst. Dyn., doi:10.5194/esd-7-681-2016, 2016a.

D'Arrigo, R., Cook, E. R., Wilson, R. J., Allan, R. and Mann, M. E.: On the variability of ENSO over the past six centuries, Geophys. Res. Lett., doi:10.1029/2004GL022055, 2005.

Ding, Y., Carton, J. A., Chepurin, G. A., Stenchikov, G., Robock, A., Sentman, L. T. and Krasting, J. P.: Ocean response to volcanic eruptions in Coupled Model Intercomparison Project 5 simulations, J. Geophys. Res. C Ocean., doi:10.1002/2013JC009780, 2014.

Driscoll, S., Bozzo, A., Gray, L. J., Robock, A. and Stenchikov, G.: Coupled Model Intercomparison Project 5 (CMIP5) simulations of climate following volcanic eruptions, J. Geophys. Res. Atmos., doi:10.1029/2012JD017607, 2012.

Eddebbar, Y. A., Rodgers, K. B., Long, M. C., Subramanian, A. C., Xie, S. P. and Keeling, R. F.: El Niño-like physical and biogeochemical ocean response to tropical eruptions, J. Clim., doi:10.1175/JCLI-D-18-0458.1, 2019.

Emile-Geay, J., Seager, R., Cane, M. A., Cook, E. R. and Haug, G. H.: Volcanoes and ENSO over the past millennium, J. Clim., doi:10.1175/2007JCLI1884.1, 2008.

Fasullo, J. T., Tomas, R., Stevenson, S., Otto-Bliesner, B., Brady, E. and Wahl, E.: The amplifying influence of increased ocean stratification on a future year without a summer, Nat. Commun., doi:10.1038/s41467-017-01302-z, 2017.

Giorgetta, M. A., Jungclaus, J., Reick, C. H., Legutke, S., Bader, J., Böttinger, M., Brovkin, V., Crueger, T., Esch, M., Fieg, K., Glushak, K., Gayler, V., Haak, H., Hollweg, H.-D., Ilyina, T., Kinne, S., Kornblueh, L., Matei, D., Mauritsen, T., Mikolajewicz, U., Mueller, W., Notz, D., Pithan, F., Raddatz, T., Rast, S., Redler, R., Roeckner, E., Schmidt, H., Schnur, R., Segschneider, J., Six, K. D., Stockhause, M., Timmreck, C., Wegner, J., Widmann, H., Wieners, K.-H., Claussen, M., Marotzke, J. and Stevens, B.: Climate and carbon cycle changes from 1850 to 2100 in MPI-ESM simulations for the Coupled Model Intercomparison Project phase 5, J. Adv. Model. Earth Syst., doi:10.1002/jame.20038, 2013.

Harshvardhan: Harshvardhan_1979_Perturbation of the Zonal Radiation Balance by a stratopsheric aerosol layer Journal of Atmospheric Science.pdf, J. Atmos. Sci., doi:10.1175/1520-0469(1979)036<1274:POTZRB>2.0.CO;2, 1979.

Iles, C. E., Hegerl, G. C., Schurer, A. P. and Zhang, X.: The effect of volcanic eruptions on global precipitation, J. Geophys. Res. Atmos., doi:10.1002/jgrd.50678, 2013.

Kang, S. M., Held, I. M., Frierson, D. M. W. and Zhao, M.: The response of the ITCZ to extratropical thermal forcing: Idealized slab-ocean experiments with a GCM, J. Clim., doi:10.1175/2007JCLI2146.1, 2008.

Khodri, M., Izumo, T., Vialard, J., Janicot, S., Cassou, C., Lengaigne, M., Mignot, J., Gastineau, G., Guilyardi, E., Lebas, N., Robock, A. and McPhaden, M. J.: Tropical explosive volcanic eruptions can trigger El Ninõ by cooling tropical Africa, Nat. Commun., doi:10.1038/s41467-017-00755-6, 2017.

Kodera, K.: Influence of volcanic eruptions on the troposphere through stratospheric dynamical processes in the Northern Hemisphere winter, J. Geophys. Res., doi:10.1029/93JD02731, 1994.

Li, J., Xie, S. P., Cook, E. R., Morales, M. S., Christie, D. A., Johnson, N. C., Chen, F., D'Arrigo, R., Fowler, A. M., Gou, X. and Fang, K.: El Niño modulations over the past seven centuries, Nat. Clim. Chang., doi:10.1038/nclimate1936, 2013.

Lim, H. G., Yeh, S. W., Kug, J. S., Park, Y. G., Park, J. H., Park, R. and Song, C. K.: Threshold of the volcanic forcing that leads the El Niño-like warming in the last millennium: results from the ERIK simulation, Clim. Dyn., doi:10.1007/s00382-015-2799-3, 2016.

Liu, F., Li, J., Wang, B., Liu, J., Li, T., Huang, G. and Wang, Z.: Divergent El Niño responses to volcanic eruptions at different latitudes over the past millennium, Clim. Dyn., doi:10.1007/s00382-017-3846-z, 2018a.

Liu, F., Xing, C., Sun, L., Wang, B., Chen, D. and Liu, J.: How Do Tropical, Northern Hemispheric, and Southern Hemispheric

https://doi.org/10.5194/esd-2020-63
Preprint. Discussion started: 19 August 2020

Volcanic Eruptions Affect ENSO Under Different Initial Ocean Conditions?, Geophys. Res. Lett., doi:10.1029/2018GL080315, 2018b.

Maher, N., McGregor, S., England, M. H. and Gupta, A. Sen: Effects of volcanism on tropical variability, Geophys. Res. Lett., doi:10.1002/2015GL064751, 2015.

Maher, N., Milinski, S., Suarez-Gutierrez, L., Botzet, M., Dobrynin, M., Kornblueh, L., Kröger, J., Takano, Y., Ghosh, R., Hedemann, C., Li, C., Li, H., Manzini, E., Notz, D., Putrasahan, D., Boysen, L., Claussen, M., Ilyina, T., Olonscheck, D., Raddatz, T., Stevens, B. and Marotzke, J.: The Max Planck Institute Grand Ensemble - Enabling the Exploration of Climate System Variability, J. Adv. Model. Earth Syst., doi:10.1029/2019MS001639, 2019.

Man, W., Zhou, T. and Jungclaus, J. H.: Effects of large volcanic eruptions on global summer climate and east asian monsoon changes during the last millennium: Analysis of MPI-ESM simulations, J. Clim., doi:10.1175/JCLI-D-13-00739.1, 2014.

Mann, M. E., Cane, M. A., Zebiak, S. E. and Clement, A.: Volcanic and solar forcing of the tropical Pacific over the past 1000 years, J. Clim., doi:10.1175/JCLI-3276.1, 2005.

McGregor, S. and Timmermann, A.: The effect of explosive tropical volcanism on ENSO, J. Clim., doi:10.1175/2010JCLI3990.1, 2011.

McGregor, S., Timmermann, A. and Timm, O.: A unified proxy for ENSO and PDO variability since 1650, Clim. Past, doi:10.5194/cp-6-1-2010, 2010.

McGregor, S., Khodry, M., Maher, N., Ohba, M., Pausata, F., Stevenson, S., The effect of strong volcanic eruptions on ENSO, AGU Books, [in press].

Milinski, S., Maher, N. and Olonscheck, D.: How large does a large ensemble need to be?, Earth Syst. Dyn. Discuss., doi:10.5194/esd-2019-70, 2019.

Ohba, M., Shiogama, H., Yokohata, T. and Watanabe, M.: Impact of strong tropical volcanic eruptions on enso simulated in a coupled gcm, J. Clim., doi:10.1175/JCLI-D-12-00471.1, 2013.

Pausata, F. S. R., Grini, A., Caballero, R., Hannachi, A. and Seland, Ø.: High-latitude volcanic eruptions in the Norwegian Earth System Model: The effect of different initial conditions and of the ensemble size, Tellus, Ser. B Chem. Phys. Meteorol., doi:10.3402/tellusb.v67.26728, 2015a.

Pausata, F. S. R., Chafik, L., Caballero, R. and Battisti, D. S.: Impacts of high-latitude volcanic eruptions on ENSO and AMOC, Proc. Natl. Acad. Sci., doi:10.1073/pnas.1509153112, 2015b.

Pausata, F. S. R., Karamperidou, C., Caballero, R. and Battisti, D. S.: ENSO response to high-latitude volcanic eruptions in the Northern Hemisphere: The role of the initial conditions, Geophys. Res. Lett., doi:10.1002/2016GL069575, 2016.

Pausata, F.S.R., Zanchettin, D., Karamperidou, C., Caballero, R., & Battisti, D. S.: ITZC shift and extratropical teleconnections drive ENSO response to volcanic eruptions, Science Advances., doi: 10.1126/sciadv.aaz5006, 2020.

Pinto, J. P., Turco, R. P. and Toon, O. B.: Self-limiting physical and chemical effects in volcanic eruption clouds, J. Geophys. Res., doi:10.1029/jd094id08p11165, 1989.

Pollack, J. B., Toon, O. B., Sagan, C., Summers, A., Baldwin, B. and Van Camp, W.: Volcanic explosions and climatic change: A theoretical assessment, J. Geophys. Res., doi:10.1029/jc081i006p01071, 1976.

Predybaylo, E., Stenchikov, G. L., Wittenberg, A. T. and Zeng, F.: Impacts of a pinatubo-size volcanic eruption on ENSO, J.

Geophys. Res., doi:10.1002/2016JD025796, 2017.

Rampino, M. R. and Self, S.: Sulphur-rich volcanic eruptions and stratospheric aerosols, Nature, doi:10.1038/310677a0, 1984.

Robock, A.: Volcanic eruptions and climate, Rev. Geophys., doi:10.1029/1998RG000054, 2000.

Robock, A. and Yuhe Liu: The volcanic signal in Goddard Institute for Space Studies three- dimensional model simulations, J. Clim., doi:10.1175/1520-0442(1994)007<0044:TVSIGI>2.0.CO;2, 1994.

Schneider, T., Bischoff, T. and Haug, G. H.: Migrations and dynamics of the intertropical convergence zone., Nature, doi:10.1038/nature13636, 2014.

Self, S. and Rampino, M. R.: The 1963-1964 eruption of Agung volcano (Bali, Indonesia), Bull. Volcanol., doi:10.1007/s00445-012-0615-z, 2012.

Self, S., Rampino, M. R., Zhao, J. and Katz, M. G.: Volcanic aerosol perturbations and strong El Niño events: No general correlation, Geophys. Res. Lett., doi:10.1029/97GL01127, 1997.

Stenchikov, G., Hamilton, K., Stouffer, R. J., Robock, A., Ramaswamy, V., Santer, B. and Graf, H. F.: Arctic Oscillation response to volcanic eruptions in the IPCC AR4 climate models, J. Geophys. Res. Atmos., doi:10.1029/2005JD006286, 2006.

Stenchikov, G. L., Kirchner, I., Robock, A., Graf, H. F., Antuña, J. C., Grainger, R. G., Lambert, A. and Thomason, L.: Radiative forcing from the 1991 Mount Pinatubo volcanic eruption, J. Geophys. Res. Atmos., doi:10.1029/98JD00693, 1998.

Stevenson, S., Otto-Bliesner, B., Fasullo, J. and Brady, E.: "El Niño Like" hydroclimate responses to last millennium volcanic eruptions, J. Clim., doi:10.1175/JCLI-D-15-0239.1, 2016.

Stevenson, S., Fasullo, J. T., Otto-Bliesner, B. L., Tomas, R. A. and Gao, C.: Role of eruption season in reconciling model and proxy responses to tropical volcanism, Proc. Natl. Acad. Sci., doi:10.1073/pnas.1612505114, 2017.

Stoffel, M., Khodri, M., Corona, C., Guillet, S., Poulain, V., Bekki, S., Guiot, J., Luckman, B. H., Oppenheimer, C., Lebas, N., Beniston, M. and Masson-Delmotte, V.: Estimates of volcanic-induced cooling in the Northern Hemisphere over the past 1,500 years, Nat. Geosci., doi:10.1038/ngeo2526, 2015.

Sun, W., Liu, J., Wang, B., Chen, D., Liu, F., Wang, Z., Ning, L. and Chen, M.: A "La Niña-like" state occurring in the second year after large tropical volcanic eruptions during the past 1500 years, Clim. Dyn., doi:10.1007/s00382-018-4163-x, 2019.

Thompson, D. W. J., Wallace, J. M., Jones, P. D. and Kennedy, J. J.: Identifying signatures of natural climate variability in time series of global-mean surface temperature: Methodology and insights, J. Clim., doi:10.1175/2009JCLI3089.1, 2009.

Timmreck, C.: Modeling the climatic effects of large explosive volcanic eruptions, Wiley Interdiscip. Rev. Clim. Chang., doi:10.1002/wcc.192, 2012.

Toohey, M., Krüger, K., Niemeier, U. and Timmreck, C.: The influence of eruption season on the global aerosol evolution and radiative impact of tropical volcanic eruptions, Atmos. Chem. Phys., doi:10.5194/acp-11-12351-2011, 2011.

Trenberth, K. E. and Dai, A.: Effects of Mount Pinatubo volcanic eruption on the hydrological cycle as an analog of geoengineering, Geophys. Res. Lett., doi:10.1029/2007GL030524, 2007.

Wilson, R., Cook, E., D'arrigo, R., Riedwyl, N., Evans, M. N., Tudhope, A. and Rob, A.: Reconstructing ENSO: The influence of method, proxy data, climate forcing and teleconnections, J. Quat. Sci., doi:10.1002/jqs.1297, 2010.

Wittenberg, A. T.: Are historical records sufficient to constrain ENSO simulations?, Geophys. Res. Lett., doi:10.1029/2009GL038710, 2009.

https://doi.org/10.5194/esd-2020-63
Preprint. Discussion started: 19 August 2020

Earth System Dynamics Discussions
Open Access
EGU

Zambri, B. and Robock, A.: Winter warming and summer monsoon reduction after volcanic eruptions in Coupled Model Intercomparison Project 5 (CMIP5) simulations, Geophys. Res. Lett., doi:10.1002/2016GL070460, 2016.

Zanchettin, D., Timmreck, C., Graf, H. F., Rubino, A., Lorenz, S., Lohmann, K., Krüger, K. and Jungclaus, J. H.: Bi-decadal variability excited in the coupled ocean-atmosphere system by strong tropical volcanic eruptions, Clim. Dyn., doi:10.1007/s00382-011-1167-1, 2012.

Zuo, M., Man, W., Zhou, T. and Guo, Z.: Different impacts of Northern, tropical, and Southern volcanic eruptions on the tropical pacific SST in the Last Millennium, J. Clim., doi:10.1175/JCLI-D-17-0571.1, 2018.

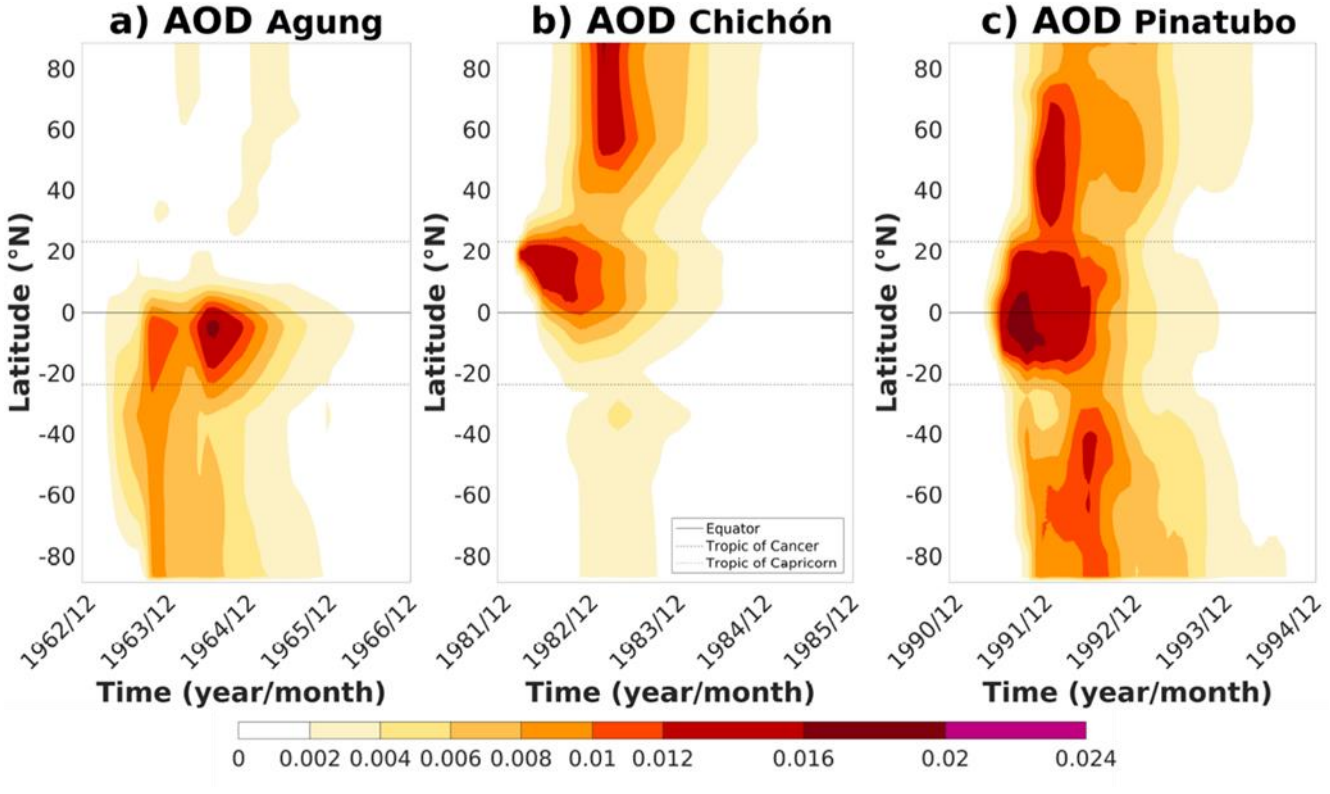

Figure 1: Evolution of the aerosol optical depth during four years for the three eruptions. The band of wavelength used is between approximatively 555 nm and 675 nm.

https://doi.org/10.5194/esd-2020-63
Preprint. Discussion started: 19 August 2020

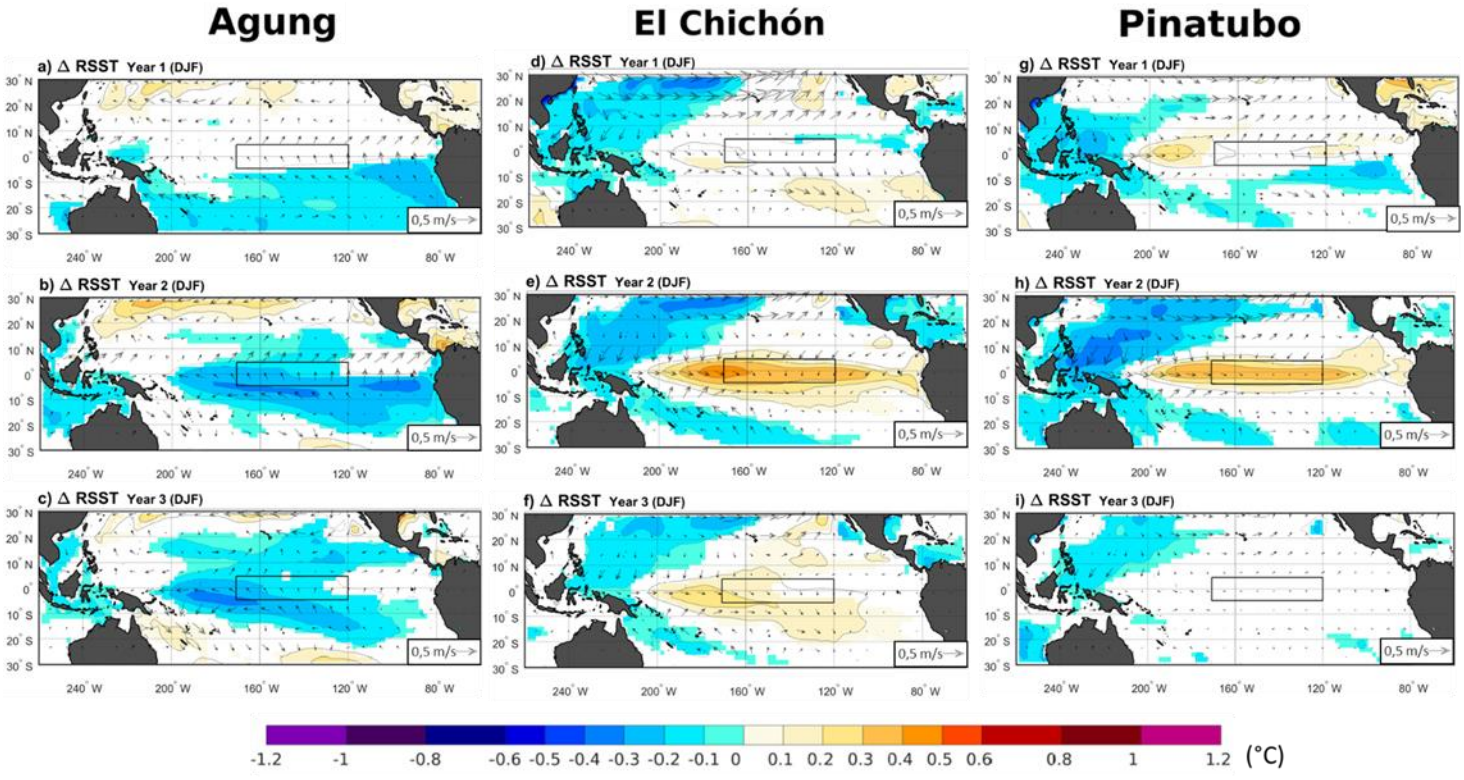

Figure 2 : Ensemble mean of changes in relative sea surface temperature (RSST) (shadings) and 10 m winds (arrows) between the volcano case and the climatology for each of the following three winter season (DJF) after the Agung (a-c), El Chichón (d-f) and the Pinatubo (g-i) eruptions. Only significant RSST changes are shaded with an approximate 95 % confidence level using a Student t-test. Contours show the RSST anomalies following the color bar scale (solid lines for positive anomalies and dashed lines lines for negative anomalies, the 0 line is omitted). The boxes indicate the Niño 3.4 area.

https://doi.org/10.5194/esd-2020-63
Preprint. Discussion started: 19 August 2020

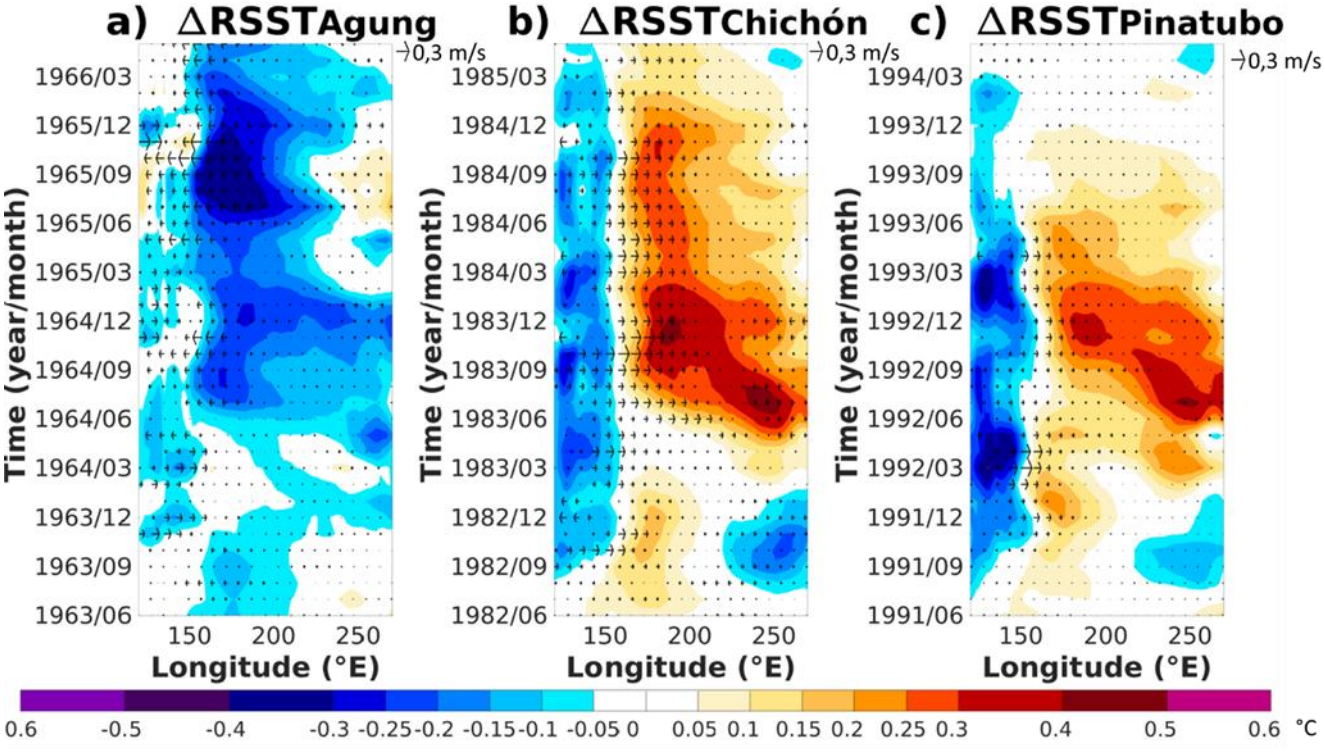

545

Figure 3: Hovmöller plot of the ensemble mean of the relative SST anomalies in the equatorial Pacific (averaged over -5 °N and 5 °N) and the change in the zonal component of the 10 m winds (m/s) for the three years following each eruption. The anomalies are calculated relative to the three years before each eruption.

https://doi.org/10.5194/esd-2020-63
Preprint. Discussion started: 19 August 2020

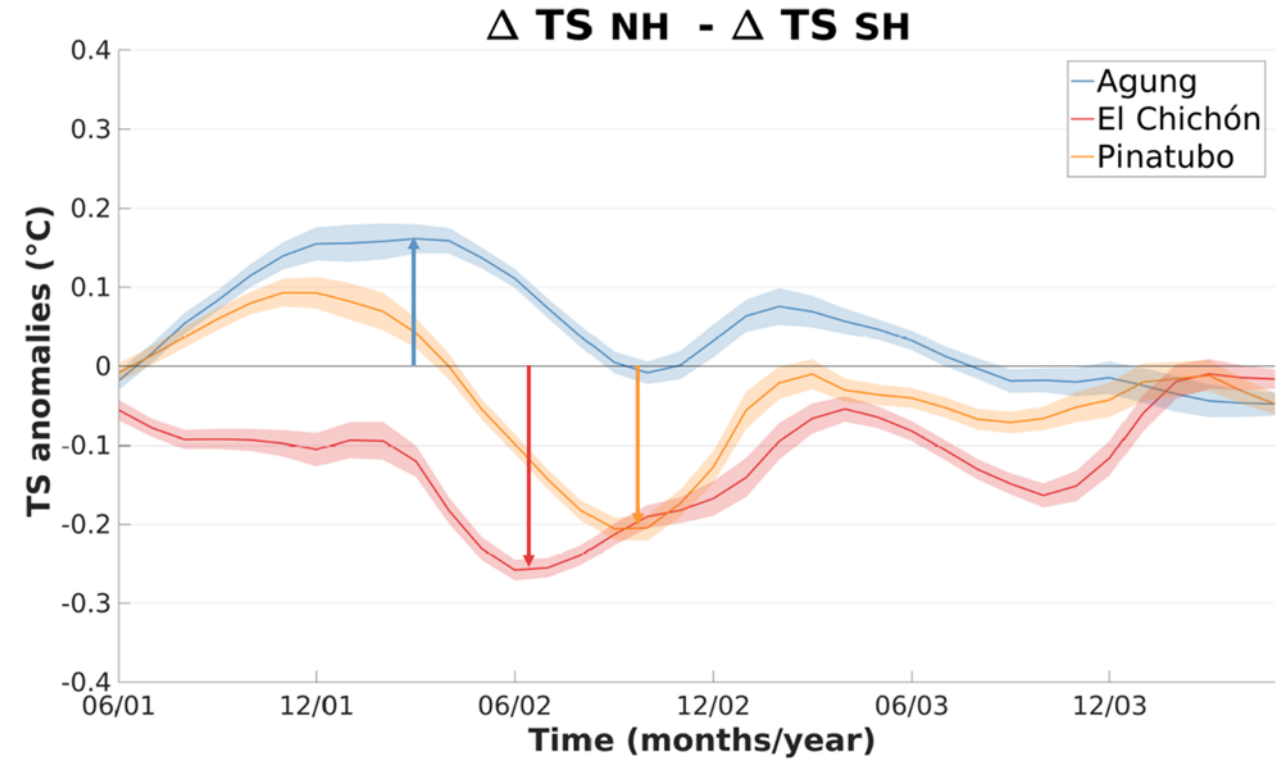

Figure 4: Evolution of the difference in the ensemble mean between the volcanically induced cooling of the SH and the NH after each eruption (ΔT_{NH} - ΔT_{SH}). Shading represents twice the standard error of the ensemble mean (i.e. ~95% confidence interval).

https://doi.org/10.5194/esd-2020-63
Preprint. Discussion started: 19 August 2020

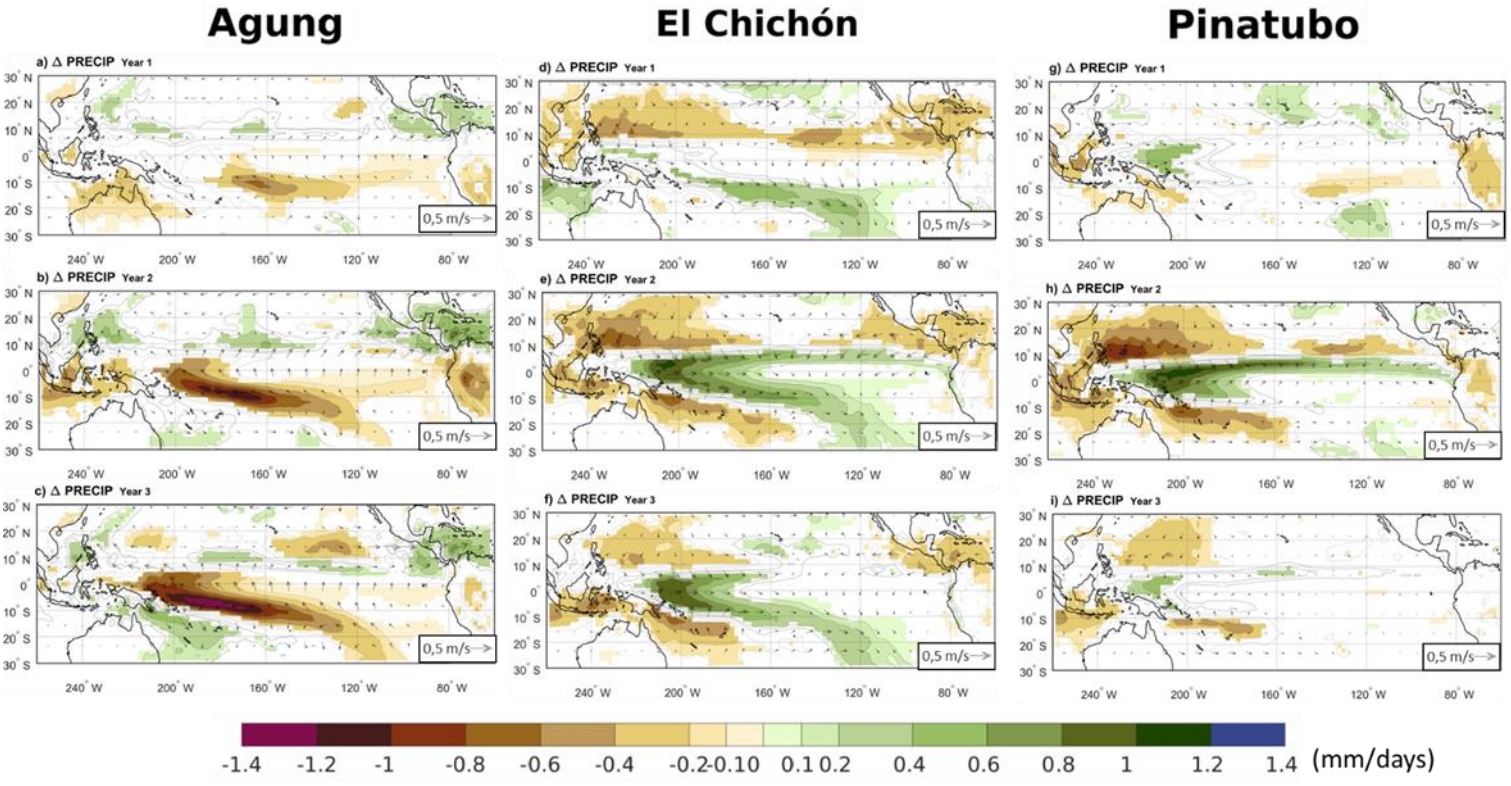

Figure 5:Change in ensemble mean precipitation and 10 m winds (arrows) between the references years and the volcano case for the three summer to winter seasons (June to February) following the Agung (a-c), El Chichón (d-f) and the Pinatubo (g-i) eruptions. Contours show the precipitation anomaly following the color bar scale (solid lines for positive anomalies and dashed lines for negative anomalies, the 0 line is omitted). Only precipitation changes that are significant at the 95% confidence level using a Student t-test are shaded.

https://doi.org/10.5194/esd-2020-63
Preprint. Discussion started: 19 August 2020

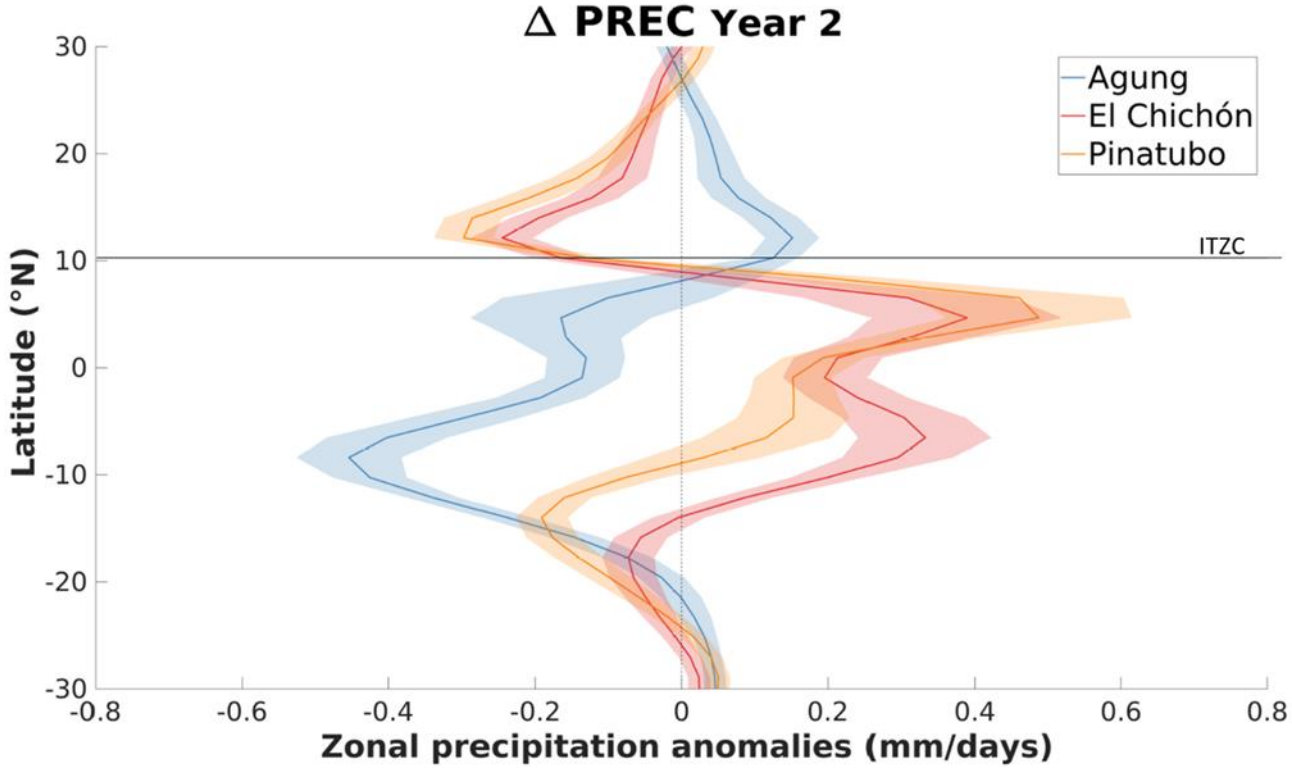

Figure 6: Ensemble mean of the zonal precipitation anomaly over the Pacific Ocean (160 °E-100 °W) between the summer to winter seasons (June to February) of the second year after each eruption and the 3-year climatology. Shading represents twice the standard error of the ensemble mean (i.e. ~95% confidence interval). The horizontal line highlights the ensemble-mean 3-year climatology position of the ITCZ (defined as the location of the zonal-average precipitation maximum).